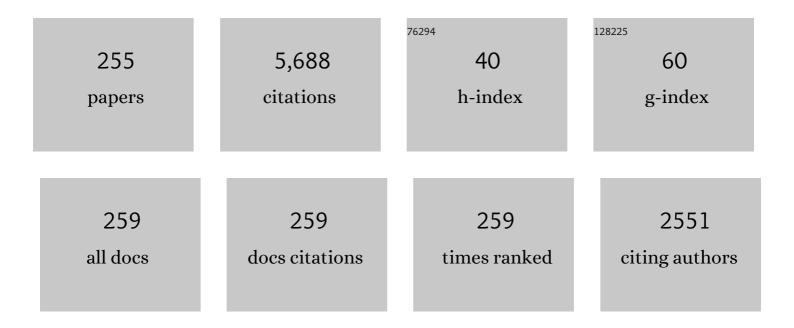
Ryosuke O Suzuki

List of Publications by Year in descending order

Source: https://exaly.com/author-pdf/1783184/publications.pdf Version: 2024-02-01



#	Article	IF	CITATIONS
1	Impact of high-temperature non-uniform degradation on fines clogging and gas flow in a coke bed. Chemical Engineering Journal, 2022, 427, 131484.	6.6	7
2	Droplet behavior analysis on inclined, highly sticky, or slippery superhydrophobic nanostructured surfaces by observation and SPH simulation. Chemical Engineering Science, 2022, 248, 117214.	1.9	5
3	Quantification of the Impact of Residual H2O on Cathodic Behavior in Molten CaCl2 Electrolysis. Journal of Sustainable Metallurgy, 2022, 8, 532-540.	1.1	4
4	Formation of Bright White Plasma Electrolytic Oxidation Films with a Uniform Maze-Like Structure by Anodizing Aluminum in Ammonium Tetraborate Solutions. Journal of the Electrochemical Society, 2022, 169, 043505.	1.3	2
5	A Sustainable Approach for Producing Ti and TiS2 from TiC. Metallurgical and Materials Transactions B: Process Metallurgy and Materials Processing Science, 2021, 52, 77-87.	1.0	6
6	High-speed galvanostatic anodizing without oxide burning using a nanodimpled aluminum surface for nanoporous alumina fabrication. Applied Surface Science, 2021, 537, 147852.	3.1	12
7	Self-ordered nanospike porous alumina fabricated under a new regime by an anodizing process in alkaline media. Scientific Reports, 2021, 11, 7240.	1.6	25
8	Synthesis of Silicon Sulfide by Using CS2 Gas. Metallurgical and Materials Transactions B: Process Metallurgy and Materials Processing Science, 2021, 52, 1379-1391.	1.0	6
9	Tantalum Metal Production Through High-Efficiency Electrochemical Reduction of TaS2 in Molten CaCl2. Journal of Sustainable Metallurgy, 2021, 7, 437-447.	1.1	7
10	Influence of sub-10Ânm anodic alumina nanowire morphology formed by two-step anodizing aluminum on water wettability and slipping behavior. Applied Surface Science, 2021, 546, 149090.	3.1	18
11	Recent Studies on Titanium Refining: 2017–2020. Materials Transactions, 2021, 62, 905-913.	0.4	9
12	Comprehensive numerical assessment of molten iron–slag trickle flow and gas countercurrent in complex coke bed by Eulerian–Lagrangian approach. Chemical Engineering Journal, 2021, 414, 128606.	6.6	8
13	Self-Ordering of Porous Anodic Alumina Fabricated by Anodizing in Chromic Acid at High Temperature. Journal of the Electrochemical Society, 2021, 168, 093501.	1.3	15
14	An Innovative Process for Production of Ti Metal Powder via TiSx from TiN. Metallurgical and Materials Transactions B: Process Metallurgy and Materials Processing Science, 2020, 51, 140-148.	1.0	14
15	Detailed modelling of packed-bed gas clogging due to thermal-softening of iron ore by Eulerian–Lagrangian approach. Chemical Engineering Journal, 2020, 392, 123643.	6.6	16
16	Visualization of TiO2 Reduction Behavior in Molten Salt Electrolysis. Metallurgical and Materials Transactions B: Process Metallurgy and Materials Processing Science, 2020, 51, 11-15.	1.0	6
17	Photoluminescence from Anodic Aluminum Oxide Formed via Etidronic Acid Anodizing and Enhancing the Intensity. Materials Transactions, 2020, 61, 1130-1137.	0.4	7
18	Initial Structural Changes of Porous Alumina Film via High-Resolution Microscopy Observations. ECS Journal of Solid State Science and Technology, 2020, 9, 044004.	0.9	10

#	Article	IF	CITATIONS
19	Characterization of the Cathodic Thermal Behavior of Molten CaCl ₂ and Its Hygroscopic Chloride Mixture During Electrolysis. Journal of the Electrochemical Society, 2020, 167, 102507.	1.3	5
20	Numerical Study of Binary Trickle Flow of Liquid Iron and Molten Slag in Coke Bed by Smoothed Particle Hydrodynamics. Processes, 2020, 8, 221.	1.3	8
21	Fabrication of a plasma electrolytic oxidation/anodic aluminum oxide multi-layer film via one-step anodizing aluminum in ammonium carbonate. Thin Solid Films, 2020, 697, 137799.	0.8	12
22	Towards a sustainable technology for production of extra-pure Ti metal: Electrolysis of sulfurized Ti(C,N) in molten CaCl2. International Journal of Minerals, Metallurgy and Materials, 2020, 27, 1635-1643.	2.4	10
23	Anodizing Aluminum and Its Alloys in Etidronic Acid to Enhance Their Corrosion Resistance in a Sodium Chloride Solution. Journal of the Electrochemical Society, 2020, 167, 121502.	1.3	6
24	Numerical Simulation of Coexisting Solid-liquid Slag Trickle Flow in a Coke Bed by the SPH Method with a Non-Newtonian Fluid Model. ISIJ International, 2020, 60, 1445-1452.	0.6	9
25	Topological Consideration of 3-D Local Void Structure for Static Holdup Site in Packed Bed. ISIJ International, 2020, 60, 1453-1460.	0.6	7
26	Numerical Approach to Comprehend for Effect of Melts Physical Properties on Iron-slag Separation Behaviour in Self-reducing Pellet. ISIJ International, 2020, 60, 2695-2704.	0.6	3
27	Nanostructure of Anodic Porous Alumina Fabricated By Galvanostatic Anodizing in Etidronic Acid. ECS Meeting Abstracts, 2020, MA2020-02, 1227-1227.	0.0	0
28	Fabrication of Sticky and Slippery Superhydrophobic Aluminum Surfaces Covered with Nanostructured Anodic Oxide. ECS Meeting Abstracts, 2020, MA2020-02, 1234-1234.	0.0	0
29	Corrosion-Resistant Porous Alumina Formed via Anodizing Aluminum in Etidronic Acid and Its Pore-Sealing Behavior in Boiling Water. Journal of the Electrochemical Society, 2019, 166, C261-C269.	1.3	36
30	Solubility of CaS in CaCl ₂ –LiCl Eutectic Melt. Materials Transactions, 2019, 60, 411-415.	0.4	5
31	Fabrication of anodic porous alumina via galvanostatic anodizing in alkaline sodium tetraborate solution and their morphology. Journal of Electroanalytical Chemistry, 2019, 846, 113152.	1.9	18
32	A Superhydrophilic Aluminum Surface with Fast Water Evaporation Based on Anodic Alumina Bundle Structures via Anodizing in Pyrophosphoric Acid. Materials, 2019, 12, 3497.	1.3	24
33	Solubility of CaS in Molten CaCl ₂ . Materials Transactions, 2019, 60, 386-390.	0.4	6
34	Nanostructural characterization of ordered gold particle arrays fabricated via aluminum anodizing, sputter coating, and dewetting. Applied Surface Science, 2019, 465, 747-753.	3.1	17
35	Structural Characterization of Anodic Porous Alumina Formed By Galvanostatic Anodizing in Etidronic Acid. ECS Meeting Abstracts, 2019, , .	0.0	0
36	Alkaline Corrosion-Resistant Anodic Aluminum Oxide Formed By Etidronic Acid Anodizing. ECS Meeting Abstracts, 2019, , .	0.0	0

#	Article	IF	CITATIONS
37	Fabrication of Sticky and Slippery Aluminum Alloys Based on Anodic Alumina Nanofibers. ECS Meeting Abstracts, 2019, , .	0.0	Ο
38	Mirror-finished superhydrophobic aluminum surfaces modified by anodic alumina nanofibers and self-assembled monolayers. Applied Surface Science, 2018, 440, 506-513.	3.1	37
39	Thermoelectric System Absorbing Waste Heat from a Steel Ladle. Journal of Electronic Materials, 2018, 47, 3238-3247.	1.0	6
40	Mathematical Analysis of the Solidification Behavior of Plain Steel Based on Solute- and Heat-Transfer Equations in the Liquid–Solid Zone. Metallurgical and Materials Transactions B: Process Metallurgy and Materials Processing Science, 2018, 49, 644-657.	1.0	3
41	Performance Analysis of Thermoelectric Modules Consisting of Square Truncated Pyramid Elements Under Constant Heat Flux. Journal of Electronic Materials, 2018, 47, 3288-3297.	1.0	5
42	DEM-SPH study of molten slag trickle flow in coke bed. Chemical Engineering Science, 2018, 175, 25-39.	1.9	30
43	Advancing and receding contact angle investigations for highly sticky and slippery aluminum surfaces fabricated from nanostructured anodic oxide. RSC Advances, 2018, 8, 37315-37323.	1.7	19
44	Holdup Characteristics of Melt in Coke Beds of Different Shapes. ISIJ International, 2018, 58, 1742-1744.	0.6	7
45	<i>(Invited) </i> Metal Production in CaCl ₂ -Based Melts. ECS Transactions, 2018, 86, 45-53.	0.3	9
46	Spontaneous colloidal metal network formation driven by molten salt electrolysis. Scientific Reports, 2018, 8, 13114.	1.6	11
47	Reduction of CaTiO ₃ by Electrolysis in the Molten Salt CaCl ₂ -CaO. Electrochemistry, 2018, 86, 82-87.	0.6	17
48	Column and film lifetimes in bubble-induced two-liquid flow. Physical Review E, 2018, 97, 062802.	0.8	8
49	Formation of Titanium Sulfide from Titanium Oxycarbonitride by CS2 Gas. Metallurgical and Materials Transactions B: Process Metallurgy and Materials Processing Science, 2018, 49, 1808-1821.	1.0	17
50	Detailed Modeling of Melt Dripping in Coke Bed by DEM – SPH. ISIJ International, 2018, 58, 282-291.	0.6	26
51	Evaluation of Coke Degradation Effect on Flow Characteristics in Packed Bed Using 3D Scanning for Rotational Mechanical Strength Test and Solid-liquid-gas Three-phase Dynamic Model Analysis. Tetsu-To-Hagane/Journal of the Iron and Steel Institute of Japan, 2018, 104, 347-357.	0.1	7
52	Hard Porous Alumina Coatings Via Etidronic Acid Anodizing. ECS Meeting Abstracts, 2018, , .	0.0	0
53	Fabrication of Sticky and Slippery Superhydrophobic Aluminum Surfaces Via Pyrophosphoric Acid Anodizing and SAM Modification. ECS Meeting Abstracts, 2018, , .	0.0	0
54	(Invited) Metal Production in CaCl2-Based Melts. ECS Meeting Abstracts, 2018, , .	0.0	0

#	Article	IF	CITATIONS
55	Nanostructural characterization of large-scale porous alumina fabricated via anodizing in arsenic acid solution. Applied Surface Science, 2017, 403, 652-661.	3.1	27
56	Thermoelectric Generation Using Counter-Flows of Ideal Fluids. Journal of Electronic Materials, 2017, 46, 5136-5144.	1.0	4
57	An SPH Study of Molten Matte–Slag Dispersion. Metallurgical and Materials Transactions B: Process Metallurgy and Materials Processing Science, 2017, 48, 1792-1806.	1.0	15
58	Morphology of lithium droplets electrolytically deposited in LiCl–KCl–Li2O melt. Electrochemistry Communications, 2017, 81, 43-47.	2.3	8
59	Branched morphology of Nb powder particles fabricated by calciothermic reduction in CaCl2 melt. Journal of Physics and Chemistry of Solids, 2017, 110, 58-63.	1.9	2
60	Capturing the nonâ€spherical shape of granular media and its trickle flow characteristics using fully‣agrangian method. AICHE Journal, 2017, 63, 2257-2271.	1.8	10
61	Performance Simulation of a Flat-Plate Thermoelectric Module Consisting of Square Truncated Pyramid Elements. Journal of Electronic Materials, 2017, 46, 2691-2696.	1.0	7
62	Advanced hard anodic alumina coatings via etidronic acid anodizing. Surface and Coatings Technology, 2017, 326, 72-78.	2.2	39
63	Superhydrophilic and superhydrophobic aluminum alloys fabricated via pyrophosphoric acid anodizing and fluorinated SAM modification. Journal of Alloys and Compounds, 2017, 725, 379-387.	2.8	34
64	Fabrication of porous tungsten oxide via anodizing in an ammonium nitrate/ethylene glycol/water mixture for visible light-driven photocatalyst. Applied Surface Science, 2017, 422, 130-137.	3.1	32
65	Thermoelectric performance using counter-flowing thermal fluids. International Journal of Hydrogen Energy, 2017, 42, 20835-20842.	3.8	10
66	Electrolytic reduction of V ₃ S ₄ in molten CaCl ₂ . Materials Transactions, 2017, 58, 371-376.	0.4	26
67	Reduction of CaTiO ₃ in Molten CaCl ₂ - as Basic Understanding of Electrolysis. Materials Transactions, 2017, 58, 341-349.	0.4	15
68	Observation of Interface Deformation in Sodium Polytungstate Solution–Silicone Oil System due to Single Rising Bubble. ISIJ International, 2017, 57, 394-396.	0.6	4
69	High-Speed Observation of Electrolytic Deposition of Liquid Lithium Droplets in LiCl-KCl Melt. ECS Meeting Abstracts, 2017, , .	0.0	0
70	Superhydrophilic and Superhydrophobic Aluminum Alloys Fabricated By Pyrophosphoric Acid Anodizing. ECS Meeting Abstracts, 2017, , .	0.0	0
71	Fabrication of Superhydrophobic Aluminum Surfaces By Pyrophosphoric Acid Anodizing and SAM Modification. ECS Meeting Abstracts, 2017, , .	0.0	0
72	Influence of Gas Injection Pipe on CO ₂ Decomposition by CaCl ₂ -CaO Molten Salt and ZrO ₂ Solid Electrolysis. Tetsu-To-Hagane/Journal of the Iron and Steel Institute of Japan, 2016, 102, 219-225.	0.1	0

#	Article	IF	CITATIONS
73	Influence of Gas Injection Pipe on CO ₂ Decomposition by CaCl ₂ –CaO Molten Salt and ZrO ₂ Solid Electrolysis. ISIJ International, 2016, 56, 2093-2099.	0.6	1
74	æ€ã,ãðãëå«å¥½2観å‰å®′会. Electrochemistry, 2016, 84, 505-505.	0.6	0
75	CO Gas Production by CO ₂ Gas Decomposition in Molten Salt Electrolysis. ECS Transactions, 2016, 75, 533-542.	0.3	3
76	Helical configuration for thermoelectric generation. Applied Thermal Engineering, 2016, 99, 352-357.	3.0	36
77	Temperature Dependence of Behavior of Interface Between Molten Sn and LiCl–KCl Eutectic Melt Due to Rising Gas Bubble. Metallurgical and Materials Transactions B: Process Metallurgy and Materials Processing Science, 2016, 47, 1532-1537.	1.0	4
78	Superhydrophilicity of a nanofiber-covered aluminum surface fabricated via pyrophosphoric acid anodizing. Applied Surface Science, 2016, 389, 173-180.	3.1	28
79	Fabrication of self-ordered porous alumina via anodizing in sulfate solutions. Materials Letters, 2016, 183, 285-289.	1.3	22
80	Structural Investigation and Indium Substitution in the Thermoelectric Mn2.7Cr0.3Si4Al2â^'x In x Series. Journal of Electronic Materials, 2016, 45, 1992-1999.	1.0	0
81	Exploration for the Self-ordering of Porous Alumina Fabricated via Anodizing in Etidronic Acid. Electrochimica Acta, 2016, 211, 515-523.	2.6	61
82	Numerical Optimization of Trapezoidal Thermoelectric Elements for Double-Pipe-Shaped Module. Journal of Electronic Materials, 2016, 45, 1358-1364.	1.0	11
83	Analysis of the Performance of Thermoelectric Modules Under Concentrated Radiation Heat Flux. Journal of Electronic Materials, 2016, 45, 1827-1835.	1.0	16
84	SPH simulations of the behavior of the interface between two immiscible liquid stirred by the movement of a gas bubble. Chemical Engineering Science, 2016, 141, 342-355.	1.9	25
85	Self-ordered Porous Alumina Fabricated via Phosphonic Acid Anodizing. Electrochimica Acta, 2016, 190, 471-479.	2.6	60
86	Growth Behavior of Anodic Alumina Nanofibers Fabricated By Pyrophosphoric Acid Anodizing and Their Hydrophilicity. ECS Meeting Abstracts, 2016, , .	0.0	0
87	CO Gas Production by CO2 Gas Decomposition in Molten Salt Electrolysis. ECS Meeting Abstracts, 2016, , .	0.0	0
88	Numerical Analysis of Blast Furnace by Discrete Element Type Model. Japanese Journal of Multiphase Flow, 2016, 30, 166-173.	0.1	0
89	Reduction of TiS2 by OS Process in CaCl2 Melt. ECS Meeting Abstracts, 2016, , .	0.0	1
90	Anodizing of Aluminum in Etidronic Acid Solution. ECS Meeting Abstracts, 2016, , .	0.0	0

#	Article	IF	CITATIONS
91	Performance Analysis of Thermoelectric Modules Using Polyhedron Elements. Materials Transactions, 2015, 56, 1092-1095.	0.4	8
92	Influence of Shape of Cohesive Zone on Gas Flow and Permeability in the Blast Furnace Analyzed by DEM-CFD Model. ISIJ International, 2015, 55, 1232-1236.	0.6	37
93	Droplet Motion on Non-smooth Solid Surface. ISIJ International, 2015, 55, 1277-1283.	0.6	9
94	CO Gas Production by Molten Salt Electrolysis from CO ₂ Gas. ISIJ International, 2015, 55, 404-408.	0.6	17
95	Characterization of Liquid Trickle Flow in Poor-Wetting Packed Bed. ISIJ International, 2015, 55, 1259-1266.	0.6	20
96	Analysis of Powder Motion in a Packed Bed of Blast Furnace Using the Discrete Element Method. ISIJ International, 2015, 55, 1313-1320.	0.6	16
97	Reduction Behavior of Packed Bed of Sinter Reduced by CO–CO ₂ –H ₂ –H ₂ O–N <sub> Gas. ISIJ International, 2015, 55, 1213-1222.</sub> 	;2 < ;/sub	>
98	Highly Ordered Anodic Alumina Nanofibers Fabricated via Two Distinct Anodizing Processes. ECS Electrochemistry Letters, 2015, 4, H14-H17.	1.9	17
99	Durability of Silicide-Based Thermoelectric Modules at High Temperatures in Air. Journal of Electronic Materials, 2015, 44, 2946-2952.	1.0	8
100	Niobium powder synthesized by calciothermic reduction of niobium hydroxide for use in capacitors. Journal of Physics and Chemistry of Solids, 2015, 78, 101-109.	1.9	10
101	Fabrication of Self-Ordered Porous Alumina via Etidronic Acid Anodizing and Structural Color Generation from Submicrometer-Scale Dimple Array. Electrochimica Acta, 2015, 156, 235-243.	2.6	98
102	Carbon Nanotube Synthesis via the Calciothermic Reduction of Carbon Dioxide with Iron Additives. ECS Solid State Letters, 2015, 4, M19-M22.	1.4	6
103	Self-Ordered Aluminum Anodizing in Phosphonoacetic Acid and Its Structural Coloration. ECS Solid State Letters, 2015, 4, P55-P58.	1.4	24
104	Optimum Exploration for the Self-Ordering of Anodic Porous Alumina Formed via Selenic Acid Anodizing. Journal of the Electrochemical Society, 2015, 162, E244-E250.	1.3	32
105	Dimensional Analysis of Thermoelectric Modules Under Constant Heat Flux. Journal of Electronic Materials, 2015, 44, 348-355.	1.0	15
106	Polymer nanoimprinting using an anodized aluminum mold for structural coloration. Applied Surface Science, 2015, 341, 19-27.	3.1	40
107	Fabrication of a novel aluminum surface covered by numerous high-aspect-ratio anodic alumina nanofibers. Applied Surface Science, 2015, 356, 54-62.	3.1	28
108	Model study of the effect of particles structure on the heat and mass transfer through the packed bed in ironmaking blast furnace. International Journal of Heat and Mass Transfer, 2015, 91, 1176-1186.	2.5	26

#	Article	IF	CITATIONS
109	Simulation Analysis of Tilted Polyhedron-Shaped Thermoelectric Elements. Journal of Electronic Materials, 2015, 44, 1469-1476.	1.0	18
110	Solubility of gaseous carbon dioxide in molten LiCl–Li2O. Fluid Phase Equilibria, 2015, 385, 48-53.	1.4	14
111	Porous Aluminum Oxide Formed by Anodizing in Various Electrolyte Species. Current Nanoscience, 2015, 11, 560-571.	0.7	64
112	Analysis of Effect of Packed Bed Structure on Liquid Flow in Packed Bed Using Moving Particle Semi-implicit Method. ISIJ International, 2015, 55, 1284-1290.	0.6	25
113	Recent Progress on Advanced Blast Furnace Mathematical Models Based on Discrete Method. ISIJ International, 2014, 54, 1457-1471.	0.6	65
114	Numerical Analysis of Carbon Monoxide–Hydrogen Gas Reduction of Iron Ore in a Packed Bed by an Euler–Lagrange Approach. Metallurgical and Materials Transactions B: Process Metallurgy and Materials Processing Science, 2014, 45, 2395-2413.	1.0	40
115	Optimization of Module Shape in Thermoelectric Power Generation. Key Engineering Materials, 2014, 617, 251-255.	0.4	Ο
116	Thermoelectric Analysis for <i>Î</i> -type Thermoelectric Module with Tilted Elements. Materials Research Innovations, 2014, 18, S4-116-S4-121.	1.0	4
117	Rapid reduction of titanium dioxide nano-particles by reduction with a calcium reductant. Journal of Physics and Chemistry of Solids, 2014, 75, 1041-1048.	1.9	25
118	Thermoelectric Analysis for Helical Power Generation Systems. Journal of Electronic Materials, 2014, 43, 1509-1520.	1.0	19
119	Fabrication of Anodic Nanoporous Alumina via Acetylenedicarboxylic Acid Anodizing. ECS Electrochemistry Letters, 2014, 3, C25-C28.	1.9	31
120	Fabrication of Anodic Porous Alumina by Squaric Acid Anodizing. Electrochimica Acta, 2014, 123, 14-22.	2.6	51
121	Thermoelectric Analysis for a Three-Dimensional Power Generator in Helical. Key Engineering Materials, 2014, 617, 260-264.	0.4	Ο
122	Growth behavior of anodic oxide formed by aluminum anodizing in glutaric and its derivative acid electrolytes. Applied Surface Science, 2014, 321, 364-370.	3.1	29
123	Fabrication of a micro-porous Ti–Zr alloy by electroless reduction with a calcium reductant for electrolytic capacitor applications. Journal of Alloys and Compounds, 2014, 586, 148-154.	2.8	7
124	Stable mesh-free moving particle semi-implicit method for direct analysis of gas–liquid two-phase flow. Chemical Engineering Science, 2014, 111, 286-298.	1.9	25
125	Using a Water Lens for Light Concentration in Thermoelectric Generation. Journal of Electronic Materials, 2014, 43, 2086-2093.	1.0	4
126	Fabrication of anodic porous alumina via anodizing in cyclic oxocarbon acids. Applied Surface Science, 2014, 313, 276-285.	3.1	57

#	Article	IF	CITATIONS
127	Self-Ordering Behavior of Anodic Porous Alumina via Selenic Acid Anodizing. Electrochimica Acta, 2014, 137, 728-735.	2.6	79
128	Multiphase Particle Simulation of Gas Bubble Passing Through Liquid/Liquid Interfaces. Materials Transactions, 2014, 55, 1707-1715.	0.4	25
129	Porous anodic oxide films on aluminum and their nanofabrication. Keikinzoku/Journal of Japan Institute of Light Metals, 2014, 64, 476-482.	0.1	4
130	Simulation of a Thermoelectric Module Having Parallelogram Elements. Materials Transactions, 2014, 55, 1219-1225.	0.4	14
131	Ultra-High Density Single Nanometer-Scale Anodic Alumina Nanofibers Fabricated by Pyrophosphoric Acid Anodizing. Scientific Reports, 2014, 4, 7411.	1.6	37
132	Effect of Powder–Liquid Interaction on Their Accumulation Behavior in Packed Bed. ISIJ International, 2014, 54, 1244-1250.	0.6	10
133	Design and Numerical Evaluation of Cascade-Type Thermoelectric Modules. Journal of Electronic Materials, 2013, 42, 1688-1696.	1.0	33
134	Fabrication of a meniscus microlens array made of anodic alumina by laser irradiation and electrochemical techniques. Electrochimica Acta, 2013, 94, 269-276.	2.6	26
135	Formation of niobium powder by electrolysis in molten salt. Electrochimica Acta, 2013, 100, 269-274.	2.6	12
136	Growth behavior of anodic porous alumina formed in malic acid solution. Applied Surface Science, 2013, 284, 907-913.	3.1	44
137	CO2 gas decomposition to carbon by electro-reduction in molten salts. Electrochimica Acta, 2013, 100, 293-299.	2.6	72
138	Production of Nb–Ti–Ni alloy in molten CaCl2. Electrochimica Acta, 2013, 100, 257-260.	2.6	9
139	Thermoelectric Generation Using Water Lenses. Journal of Electronic Materials, 2013, 42, 1960-1965.	1.0	6
140	Aluminum bulk micromachining through an anodic oxide mask by electrochemical etching in an acetic acid/perchloric acid solution. Microelectronic Engineering, 2013, 111, 14-20.	1.1	33
141	Rapid fabrication of self-ordered porous alumina with 10-/sub-10-nm-scale nanostructures by selenic acid anodizing. Scientific Reports, 2013, 3, 2748.	1.6	94
142	Decomposition of CO2 Gas in CaCl2-CaO and LiCl-Li2O Molten Salts. ECS Transactions, 2013, 50, 443-450.	0.3	3
143	New n-type Silicide Thermoelectric Material with High Oxidation Resistance. Materials Research Society Symposia Proceedings, 2013, 1490, 103-112.	0.1	3
144	Effect of High Reactivity Coke for Mixed Charge in Ore Layer on Reaction Behavior of Each Particle in Blast Furnace. ISIJ International, 2013, 53, 1770-1778.	0.6	37

#	Article	IF	CITATIONS
145	Influence of Physical Properties of Melt on Liquid Dripping in Packed Bed Analyzed by MPS Method. ISIJ International, 2013, 53, 590-597.	0.6	18
146	Thermoelectric properties of n-type Mn3â^'xCrxSi4Al2 in air. Journal of Applied Physics, 2012, 112, 073713.	1.1	11
147	Power generation using the fluids blown perpendicular to the TE panel. , 2012, , .		3
148	Dimensional optimization of thermoelectric modules for solar power generation. , 2012, , .		4
149	Wettability Model Considering Three-Phase Interfacial Energetics in Particle Method. Materials Transactions, 2012, 53, 662-670.	0.4	20
150	CO ₂ decomposition using electrochemical process in molten salts. Journal of Physics: Conference Series, 2012, 379, 012038.	0.3	10
151	Numerical Simulation of Dripping Behavior of Droplet in Packed Bed Using Particle Method. ISIJ International, 2012, 52, 1565-1573.	0.6	28
152	Analysis of Heat and Mass Transfer in a Packed Bed by Considering Particle Arrangement. Tetsu-To-Hagane/Journal of the Iron and Steel Institute of Japan, 2012, 98, 341-350.	0.1	10
153	Effects of Fluid Directions on Heat Exchange in Thermoelectric Generators. Journal of Electronic Materials, 2012, 41, 1766-1770.	1.0	19
154	Gas–solid flow simulation of fines clogging a packed bed using DEM–CFD. Chemical Engineering Science, 2012, 71, 274-282.	1.9	44
155	Dynamic Analysis of Gas and Solid Flows in Blast Furnace with Shaft Gas Injection by Hybrid Model of DEM-CFD. ISIJ International, 2011, 51, 51-58.	0.6	41
156	Effect of Sulfur on the TTT Diagram of CaO–Al2O3 Slag at Eutectic Composition. ISIJ International, 2011, 51, 1974-1981.	0.6	2
157	Simultaneous Three-dimensional Analysis of Gas–Solid Flow in Blast Furnace by Combining Discrete Element Method and Computational Fluid Dynamics. ISIJ International, 2011, 51, 41-50.	0.6	65
158	Computational Simulation of Thermoelectric Generators in Marine Power Plants. Materials Transactions, 2011, 52, 1549-1552.	0.4	28
159	Calciothermic reduction of NiO by molten salt electrolysis of CaO in CaCl2 melt. Electrochimica Acta, 2011, 56, 8422-8429.	2.6	45
160	Experimental Study of a Thermoelectric Generation System. Journal of Electronic Materials, 2011, 40, 744-752.	1.0	29
161	Design methodology of large-scale thermoelectric generation: A hierarchical modeling approach in SPICE. , 2011, , .		5
162	Atmosphere Controlled Hot Thermocouple Method and Crystallization Phenomenon of CaO–Al2O3 Eutectic Slag. ISIJ International, 2011, 51, 1967-1973.	0.6	5

#	Article	IF	CITATIONS
163	Thermoelectric Properties of Zr3Mn4Si6 and TiMnSi2. Journal of Electronic Materials, 2010, 39, 2017-2022.	1.0	1
164	Multi-Layered Thermoelectric Power Generator. Advances in Science and Technology, 2010, 74, 1-8.	0.2	0
165	Direct Production of Ti–29Nb–13Ta–4.6Zr Biomedical Alloy from Oxide Mixture in Molten CaCl[sub 2]. Journal of the Electrochemical Society, 2010, 157, E117.	1.3	19
166	Electronic structure and magnetic properties of monoclinic <mml:math xmlns:mml="http://www.w3.org/1998/Math/MathML" display="inline"><mml:mrow><mml:mi>î²</mml:mi><mml:msub><mml:mrow><mml:mtext>-Cu</mml:mtext><!--<br-->A<mml:math <br="" xmlns:mml="http://www.w3.org/1998/Math/MathML">display="inline"><mml:mtp: 1998="" math="" mathml"<="" td="" www.w3.org=""><td>mn lımrov</td><td>w> ଥଞ୍ଚml:mn></td></mml:mtp:></mml:math></mml:mrow></mml:msub></mml:mrow></mml:math 	m n lı mrov	w> ଥଞ୍ଚml:mn>
167	Direct Reduction of Liquid V2O5 in Molten CaCl2. ECS Transactions, 2009, 16, 255-264.	0.3	3
168	Calciothermic Reduction of TiCl4 Gas during the Electrolysis of CaCl2 Melt. ECS Transactions, 2009, 16, 265-270.	0.3	2
169	Influence of Current Density on the Reduction of TiO ₂ in Molten Salt (CaCl ₂ + CaO). Materials Transactions, 2009, 50, 2704-2708.	0.4	14
170	Performance analysis of a double-pass thermoelectric solar air collector. Solar Energy Materials and Solar Cells, 2008, 92, 1105-1109.	3.0	40
171	Synthesis of Higher Chromium Oxides Using Ozone Gas. Journal of the American Ceramic Society, 2008, 91, 1148-1154.	1.9	9
172	Direct reduction of vanadium oxide in molten CaCl ₂ . Institutions of Mining and Metallurgy Transactions Section C: Mineral Processing and Extractive Metallurgy, 2008, 117, 108-112.	0.6	3
173	Direct Reduction of Vanadium Oxide in the Molten Calcium Chloride. Nippon Kinzoku Gakkaishi/Journal of the Japan Institute of Metals, 2008, 72, 181-187.	0.2	5
174	Synthesis of Ti-6Al-4V Alloy by the Electrolysis of Molten CaCl2+CaO. Nippon Kinzoku Gakkaishi/Journal of the Japan Institute of Metals, 2008, 72, 921-927.	0.2	8
175	Influence of Current Density to Direct Reduction of TiO2 in Molten CaCl2. Nippon Kinzoku Gakkaishi/Journal of the Japan Institute of Metals, 2008, 72, 916-920.	0.2	3
176	Direct Reduction of Vanadium Oxide in Molten CaCl2. ECS Transactions, 2007, 3, 347-356.	0.3	12
177	Thermoelectric Properties and Phase Transition of (Zn <i>_x</i> Cu _{2−<i>x</i>})V&l Materials Transactions, 2007, 48, 2094-2099.	t; SolB >	;2& h ;/SUB&g
178	Thermoelectric Properties and Phase Transition of (ZnxCu2-x)V2O7. Funtai Oyobi Fummatsu Yakin/Journal of the Japan Society of Powder and Powder Metallurgy, 2007, 54, 356-361.	0.1	3
179	Direct reduction processes for titanium oxide in molten salt. Jom, 2007, 59, 68-71.	0.9	58
180	Mathematic Simulation on Power Generation by Roll Cake Type of Thermoelectric Cylinders. , 2006, , .		0

#	Article	IF	CITATIONS
181	Recycling of rare earth magnet scraps: Carbon and oxygen removal from Nd magnet scraps. Journal of Alloys and Compounds, 2006, 408-412, 1377-1381.	2.8	32
182	The Phase Equilibria and Seebeck Coefficient of (Co,M) ₃ AlC (M=Fe or Ni). Materials Transactions, 2006, 47, 1422-1427.	0.4	12
183	Chromia Coating on Iron Formed from CrO3 in Ozone. Oxidation of Metals, 2006, 65, 39-52.	1.0	4
184	Calciothermic reduction of TiO2 and in situ electrolysis of CaO in the molten CaCl2. Journal of Physics and Chemistry of Solids, 2005, 66, 461-465.	1.9	139
185	Silicide coating on refractory metals in molten salt. Journal of Physics and Chemistry of Solids, 2005, 66, 526-529.	1.9	39
186	Tantalum and niobium powder preparation from their oxides by calciothermic reduction in the molten CaCl2. Journal of Physics and Chemistry of Solids, 2005, 66, 466-470.	1.9	62
187	Direct Synthesis of TiCr ₂ Powder by Calciothermic Co-reduction of their Oxides in Molten CaCl ₂ . Electrochemistry, 2005, 73, 724-729.	0.6	9
188	Formation of broccoli-like morphology of tantalum powder. Journal of Alloys and Compounds, 2005, 389, 310-316.	2.8	24
189	Dielectric properties of tantalum powder with broccoli-like morphology. Journal of Alloys and Compounds, 2005, 392, 225-230.	2.8	14
190	Preparation of Hydrogen Storage Alloys from the Oxides by Calcium Co-Reduction in Molten CaCl2. ECS Proceedings Volumes, 2004, 2004-24, 1006-1016.	0.1	0
191	Thermoelectric Properties of Fe2TiAl Heusler Alloys ChemInform, 2004, 35, no.	0.1	0
192	Mathematic simulation on power generation by roll cake type of thermoelectric tubes. Journal of Power Sources, 2004, 132, 266-274.	4.0	20
193	Mathematic simulation on power generation by roll cake type of thermoelectric double cylinders. Journal of Power Sources, 2004, 133, 277-285.	4.0	31
194	Thermoelectric properties of Fe2TiAl Heusler alloys. Journal of Alloys and Compounds, 2004, 377, 38-42.	2.8	51
195	Direct synthesis of the hydrogen storage V–Ti alloy powder from the oxides by calcium co-reduction. Journal of Alloys and Compounds, 2004, 385, 173-180.	2.8	41
196	Reduction of TiO ₂ in Molten CaCl ₂ by Ca Deposited during CaO Electrolysis. Materials Transactions, 2004, 45, 1665-1671.	0.4	61
197	Calciothermic reduction of titanium oxide in molten CaCl2. Metallurgical and Materials Transactions B: Process Metallurgy and Materials Processing Science, 2003, 34, 277-285.	1.0	115
198	Calciothermic reduction of titanium oxide and in-situ electrolysis in molten CaCl2. Metallurgical and Materials Transactions B: Process Metallurgy and Materials Processing Science, 2003, 34, 287-295.	1.0	216

#	Article	IF	CITATIONS
199	Mathematical simulation of thermoelectric power generation with the multi-panels. Journal of Power Sources, 2003, 122, 201-209.	4.0	62
200	Mathematic simulation on thermoelectric power generation with cylindrical multi-tubes. Journal of Power Sources, 2003, 124, 293-298.	4.0	43
201	Conversion of unused heat energy to electricity by means of thermoelectric generation in condenser. IEEE Transactions on Energy Conversion, 2003, 18, 330-334.	3.7	65
202	é,"åf性溶èžåj©ã«ã, ã, é,åŒ−ãfē, jãf³ã®ç>´æŽ¥é,"åf. Materia Japan, 2002, 41, 28-31.	0.1	22
203	Recycling of Rare Earth Magnet Scraps Part III Carbon Removal from Nd Magnet Grinding Sludge under Vacuum Heating. Materials Transactions, 2002, 43, 256-260.	0.4	27
204	NbSi2 coating on niobium using molten salt. Journal of Alloys and Compounds, 2002, 336, 280-285.	2.8	69
205	A new concept for producing Ti sponge: Calciothermic reduction. Jom, 2002, 54, 59-61.	0.9	248
206	A New Concept of Sponge Titanium Production by Calciothermic Reduction of Titanium Oxide in the Molten CaCl2. ECS Proceedings Volumes, 2002, 2002-19, 810-821.	0.1	8
207	Seebeck coefficient of (Fe,V)3Al alloys. Journal of Alloys and Compounds, 2001, 329, 63-68.	2.8	46
208	Recycling of Rare Earth Magnet Scraps: Part I Carbon Removal by High Temperature Oxidation. Materials Transactions, 2001, 42, 2487-2491.	0.4	32
209	Electroless coating of Fe ₃ Si on steel in the molten salt. Steel Research = Archiv Für Das Eisenhüttenwesen, 2000, 71, 130-137.	0.2	14
210	Growth of Fe3Si layer deposited from the molten salt. Steel Research = Archiv Für Das Eisenhüttenwesen, 2000, 71, 138-143.	0.2	8
211	MoSi2 coating on molybdenum using molten salt. Journal of Alloys and Compounds, 2000, 306, 285-291.	2.8	86
212	Thermoelectric Properties of Fe-Mn-Si Alloys and Compound Fe ₃ Si doped with Mn and V. Nippon Kinzoku Gakkaishi/Journal of the Japan Institute of Metals, 1999, 63, 1435-1442.	0.2	4
213	Titanium powder prepared by magnesiothermic reduction of Ti2+ in molten salt. Metallurgical and Materials Transactions B: Process Metallurgy and Materials Processing Science, 1999, 30, 403-410.	1.0	23
214	Solid-state deoxidation of niobium by vacuum-deposited titanium. Journal of Alloys and Compounds, 1999, 284, 222-227.	2.8	2
215	Calcium-deoxidation of niobium and titanium in Ca-saturated CaCl2 molten salt. Journal of Alloys and Compounds, 1999, 288, 173-182.	2.8	92
216	Use of Ozone to Prepare Silver Oxides. Journal of the American Ceramic Society, 1999, 82, 2033-2038.	1.9	55

#	Article	IF	CITATIONS
217	Thermodynamic description of the Pb-O system. Journal of Phase Equilibria and Diffusion, 1998, 19, 213-233.	0.3	79
218	Titanium powder production by TiCl4 gas injection into magnesium through molten salts. Metallurgical and Materials Transactions B: Process Metallurgy and Materials Processing Science, 1998, 29, 1167-1174.	1.0	22
219	Thermoelectric power generation: Converting low-grade heat into electricity. Jom, 1998, 50, 49-51.	0.9	46
220	Solid state deoxidation of niobium by calcium and magnesium. Journal of Alloys and Compounds, 1998, 266, 247-254.	2.8	18
221	Thermoelectric properties of the Fe-Al and Fe-Al-Si alloys for thermoelectric generation utilising low-temperature heat sources. Steel Research = Archiv Für Das Eisenhüttenwesen, 1998, 69, 387-390.	0.2	10
222	Experimental Phase Diagram in the Ag u ₂ O uO System. Journal of the American Ceramic Society, 1998, 81, 2181-2187.	1.9	34
223	Experimental Phase Equilibria in the PbOx aO System. Journal of the American Ceramic Society, 1998, 81, 2493-2496.	1.9	4
224	Seebeck Effect of Fe-Al-Si Alloy and Low Temperature Thermoelectric Properties. Tetsu-To-Hagane/Journal of the Iron and Steel Institute of Japan, 1998, 84, 154-158.	0.1	8
225	Removal of oxygen and nitrogen from niobium by external gettering. Journal of Alloys and Compounds, 1997, 248, 251-258.	2.8	10
226	Iron-based Element for Low Temperature Thermoelectric Generator. Tetsu-To-Hagane/Journal of the Iron and Steel Institute of Japan, 1997, 83, 157-161.	0.1	13
227	Quantitative SIMS Analysis of Trace Metallic Impurities in High Purity Copper. Nippon Kinzoku Gakkaishi/Journal of the Japan Institute of Metals, 1996, 60, 290-294.	0.2	2
228	Quantitative SIMS Analysis of Mo in Ti-Dilute Mo Alloys Using Isotopic Abundance. Nippon Kinzoku Gakkaishi/Journal of the Japan Institute of Metals, 1996, 60, 406-411.	0.2	1
229	Elimination of Copper from Molten Steel by Ammonia Gas Blowing. Tetsu-To-Hagane/Journal of the Iron and Steel Institute of Japan, 1996, 82, 135-140.	0.1	9
230	Elimination of copper from the molten steel by NH3blowing under reduced pressure. Steel Research = Archiv Für Das Eisenhüttenwesen, 1995, 66, 372-376.	0.2	13
231	Local Quantitative SIMS Analysis of Small Amount of Oxygen in Titanium. Nippon Kinzoku Gakkaishi/Journal of the Japan Institute of Metals, 1995, 59, 973-977.	0.2	4
232	Phase Equilibria in the Sr-Ca-Cu-O system. , 1995, , 357-360.		2
233	Oxidation Resistant Coating for Niobium by Combining Hot Dipping in Molten Aluminum Coating and Anodic Oxidation. Nippon Kinzoku Gakkaishi/Journal of the Japan Institute of Metals, 1995, 59, 967-972.	0.2	6
234	Thermodynamics and Phase Equilibria in the CaCuO System. Journal of the American Ceramic Society, 1994, 77, 41-48.	1.9	20

#	Article	IF	CITATIONS
235	Phase Equilibria and Thermodynamics in the Sr-Cu-O and Ca-Cu-O Systems. , 1993, , 399-402.		0
236	Thermodynamics and Phase Equilibria in the SrCuO System. Journal of the American Ceramic Society, 1992, 75, 2833-2842.	1.9	49
237	Compositional range of the Bi2Sr2CaCu2OxHTc-superconductor and its surrounding phases. Physica C: Superconductivity and Its Applications, 1992, 203, 299-314.	0.6	72
238	Production of Extra Low Oxygen Titanium by Calcium-Halide Flux Deoxidation. Tetsu-To-Hagane/Journal of the Iron and Steel Institute of Japan, 1991, 77, 93-99.	0.1	65
239	Thermodynamic Properties of Dilute Titanium-Oxygen Solid Solution in Beta Phase. Materials Transactions, JIM, 1991, 32, 485-488.	0.9	109
240	Thermodynamics of Y ₂ Cu ₂ O ₅ and YCuO ₂ and Phase Equilibria in the Ba–Y–Cu–O System. Materials Transactions, JIM, 1990, 31, 1078-1084.	0.9	11
241	Preparation of intermetallic compounds by the calciothermic reaction Journal of Advanced Science, 1989, 1, 69-73.	0.1	6
242	Processes to produce superconducting Nb3Sn powders from Nb-Sn oxide. Journal of Materials Science, 1987, 22, 1999-2005.	1.7	10
243	Metastable solid solubility limit of carbon in the Ni-C system. Journal of Materials Science Letters, 1985, 4, 872-875.	O.5	24
244	Unidirectional crystallization of amorphous Te-Ge alloy. Journal of Materials Science Letters, 1985, 4, 1495-1497.	0.5	1
245	KINETICS OF ENTHALPY RELAXATION IN METALLIC GLASSES. , 1985, , 651-654.		0
246	Crystallization of Amorphous Alloys. Tetsu-To-Hagane/Journal of the Iron and Steel Institute of Japan, 1984, 70, 1828-1832.	0.1	0
247	SAXS study on crystallization of an amorphous Pd76Au6Si18 alloy. Journal of Materials Science, 1984, 19, 1476-1485.	1.7	9
248	Enthalphy relaxation of some metallic glasses near T g. Journal of Non-Crystalline Solids, 1984, 61-62, 1003-1008.	1.5	27
249	Formation and crystallization of Al-Fe-Si amorphous alloys. Journal of Materials Science, 1983, 18, 1195-1201.	1.7	78
250	DSC study of Pd76Au6Si18 amorphous alloy. Journal of Materials Science Letters, 1982, 1, 127-130.	0.5	10
251	SAXS study on the structure and crystallization of amorphous metallic alloys. Colloid and Polymer Science, 1981, 259, 677-682.	1.0	13
252	Study of the structure and crystallization of an Fe-17 at % B amorphous alloy. Journal of Materials Science, 1981, 16, 957-967.	1.7	39

#	Article	IF	CITATIONS
253	Mathematical simulation of thermoelectric power generation with the multi-flat-panels. , 0, , .		2
254	Light-Concentration Characteristic of Water Lens and its Application to Thermoelectric Generation. Key Engineering Materials, 0, 617, 247-250.	0.4	0
255	Analysis of the Solidus Temperature of Multicomponent Steel by a Finite Thickness Model with Heat- and Solute-Transfer Equations in the Solid–Liquid Zone. Metallurgical and Materials Transactions B: Process Metallurgy and Materials Processing Science, 0, , 1.	1.0	0